DOI: 10.1046/j.1464–5491.2003.01085.x

Automated detection of diabetic retinopathy in digital retinal images: a tool for diabetic retinopathy screening

D. Usher*†, M. Dumskyj§, M. Himaga*, T. H. Williamson†, S. Nussey‡ and J. Boyce*

*Department of Physics, King's College, †Department of Ophthalmology, St Thomas' Hospital, ‡Department of Oncology, Gastroenterology, Endocrinology and Metabolism, St George's Hospital Medical School, and §Department of Endocrinology, Royal Free Hospital, London, UK

Accepted 22 May 2003

Abstract

Aims To develop a system to detect automatically features of diabetic retinopathy in colour digital retinal images and to evaluate its potential in diabetic retinopathy screening.

Methods Macular centred 45° colour retinal images from 1273 patients in an inner city diabetic retinopathy screening programme. A system was used involving pre-processing to standardize colour and enhance contrast, segmentation to reveal possible lesions and classification of lesions using an artificial neural network. The system was trained using a subset of images from 500 patients and evaluated by comparing its performance with a human grader on a test set of images from 773 patients.

Results Maximum sensitivity for detection of any retinopathy on a per patient basis was 95.1%, accompanied by specificity of 46.3%. Specificity could be increased as far as 78.9% but was accompanied by a fall in sensitivity to 70.8%. At a setting with 94.8% sensitivity and 52.8% specificity, no cases of sight-threatening retinopathy were missed (retinopathy warranting immediate ophthalmology referral or re-examination sooner than 1 year by National Institute for Clinical Excellence criteria). If the system was implemented at 94.8% sensitivity setting over half the images with no retinopathy would be correctly identified, reducing the need for a human grader to examine images in 1/3 of patients.

Conclusion This system could be used when screening for diabetic retinopathy. At 94.8% sensitivity setting the number of normal images requiring examination by a human grader could be halved.

Diabet. Med. 21, 84–90 (2004)

Keywords diabetic retinopathy, screening, image analysis, neural network

Introduction

Diabetic retinopathy (DR) remains the commonest cause of blindness in the working age population of the developed world [1]. Effective treatment is available if the condition is detected early, before visual symptoms occur [2,3]. The need for a comprehensive DR screening programme has long been recognized [4] and it is now feasible [5–15]. The UK National Screening Committee has recommended digital photography as the preferred modality for any newly established DR screening programme [16]. A major cost of screening by this method comprises the salaries of staff trained to review retinal photographs [17]. Automated image processing may reduce the number of images requiring human grading with associated cost reductions [18].

A large number of studies have reported interesting preliminary results for varying approaches to automated detection of DR [19–26], but few have evaluated large numbers of images.

Automated techniques for detecting and counting microaneurysms in digitized fluorescein angiograms have given good results compared with human observers [19,22,23]. However, angiography with intravenous fluorescein is too invasive to be used during screening and the role of oral fluorescein is uncertain [27].

Correspondence to: Mr Tom H. Williamson, Department of Ophthalmology, St Thomas' Hospital, London SE1 7EH, UK. E-mail: tom@retinasurgery.co.uk

Hipwell *et al*. adapted a technique originally developed for fluorescein angiograms, and applied it to microaneurysm detection in digitally acquired red-free retinal images [20]. The system was tested on a large sample of previously unseen images designed to mimic a screening scenario. Sensitivity and specificity of 85% and 76% for detection of any retinopathy on a per patient basis was achieved.

Lee *et al*. used digitized colour retinal images and aimed to detect haemorrhages, microaneurysms, exudates and cotton wool spots [26]. They report high levels of agreement between their system and human graders on a lesion by lesion basis, but do not report overall sensitivity and specificity on a per patient basis.

This paper describes the development of a system to detect microaneurysms, haemorrhages and exudates in colour retinal images. The primary aim of the system was to detect any diabetic retinopathy in images from a diabetic screening population with the secondary aim of detecting all patients with sight-threatening disease. If successful, this would allow the removal of normal images from a dataset of screened images with the remainder sent to human observers for grading. The system was evaluated on a large sample of unselected digitally acquired low-resolution images from an existing DR screening programme.

Methods

Study images and retinopathy grading

Retinal images from 1273 consecutive patients were obtained from an existing clinical diabetic retinopathy screening service. The number of patients was chosen to optimize artificial neural network training of the less common exudates and also to aim for standard errors for sensitivity data of 0.01–0.03 (assuming a sensitivity of 0.9). Images comprised one 45° macular centred field from each eye, and were masked and identified only by patient number (1–1273). They were obtained using a Topcon TRC-NW5S non-mydriatic retinal camera (Topcon UK, Newbury, UK) with a Sony digital video attachment, providing images of 570×570 pixels in 32-bit colour in JPEG format. Mydriasis was routinely performed using 1% Tropicamide.

Retinopathy grading was performed on all images by an experienced clinical research fellow (a diabetologist with previous research training in diabetic retinopathy and an interest in diabetic retinal screening, who's performance was audited by a consultant ophthalmologist). The grading scheme from the EURODIAB protocol was used with a set of standard images enabling classification of retinopathy into the categories given in Table 1 [28]. This protocol provides a proven method of classifying the severity of retinopathy. However, it does not define sight-threatening maculopathy, which is the commonest cause of visual loss in Type 2 diabetes. All false-negative results were therefore later reviewed and classified using the National Institute for Clinical Excellence (NICE) guidelines for Type 2 diabetes (www.nice.org.uk), according to whether review earlier than 12 months for repeat photography would have been advised. Specifically, this amounts to patients with exudates within one disc diameter of the fovea for whom ophthalmology referral is advised, and those with scattered exudates outside the peri-foveal area, for whom repeat photography in 3–6 months is advised. The final definition of sight-threatening retinopathy for this study was therefore the presence of EURODIAB grade 3 or 5 retinopathy (preproliferative or proliferative) or sight-threatening maculopathy by NICE guidelines.

At present automated determination of image gradability is not fully developed. Images judged ungradable by the clinician were therefore manually excluded from the analysis.

System development, training, preliminary testing and validation were carried out using images from patients 1–500. A full evaluation of system performance was then performed

Table 1 Retinopathy grading of study patients using the EURODIAB protocol

	Training set (patients 1–500)		Evaluation set (patients 501–1273)	
Retinopathy grade by patient*	*n*	%†	*n*	%†
0 No abnormality	156	33.1	243	34.6
1 Minimal non-proliferative	133	28.2	195	27.7
2 Moderate non-proliferative	8	1.7	30	4.3
3 Pre-proliferative	11	2.3	30	4.3
4 Photocoagulated only‡	3	0.6	3	0.4
5 Proliferative	4	0.8	9	1.3
Drusen only	127	27.0	168	23.9
Other only§	29	6.2	25	3.6
Ungradable	29		70	
Prevalence of retinopathy		33.7		38.0

The training set was used to train the artificial neural networks and the evaluation set used to test the performance of the classification. The data show a similar prevalence of retinopathy.
*Where eyes differed in grade the highest was taken as the patient retinopathy grade.
†Percentage figures, including retinopathy prevalence, are calculated as percentage of gradable images.
‡Where active retinopathy was present in a previously photocoagulated eye the grade of the active retinopathy has been assigned.
§Other abnormalities included pigment spots and abnormal disc appearances.

using the previously unseen images from patients 501–1273. As a blinding procedure grading by the EURODIAB protocol was completed on all images 4 months before system training took place. Table 1 shows the retinal characteristics of the patients in the study. As images were obtained from an existing screening service no data on age, ethnicity, duration or type of diabetes was available. However, the population served is from a South London inner city area, with a high proportion of patients of South Asian and Afro-Caribbean origin, in whom Type 2 diabetes accounts for most cases.

Image processing and classification

Image processing comprised four main phases: (i) pre-processing; (ii) identification of normal structures; (iii) identification of candidate lesions; (iv) extraction of candidate lesion features.

Classification was a two-phase process comprising: (i) classification of each candidate lesion as true lesion or noise using an artificial neural network; (ii) classification of images and patients as normal or abnormal using mathematical rules.

These steps are described in further detail below.

Pre-processing

Contrast showed a tendency to diminish towards the edge of the images. Intensity varied between images, and there were considerable colour variations due to differing ethnic origin. Locally adaptive contrast enhancement was therefore applied to the intensity band to enhance contrast and normalize intensity. To simplify subsequent processing colour was standardized towards that of a preselected 'typical' normal fundus image [27].

Identification of normal structures

The optic disc comprises a bright structure traversed by dark blood vessels, and can be identified as the area of maximum contrast in the image. This is achieved by producing a variance image and identifying the peak intensities within this image [29].

A number of methods for detection of the vascular tree in re-tinal images have been described [30]. In this study Gaussian shaped multiresolution-matched filters in 16 orientations were employed.

Identification of candidate lesions

Bright lesions (exudates) were extracted using a combination of recursive region growing (RRG) and adaptive intensity thresholding (AIT) as previously described.

Dark lesions were extracted in a similar way but with the additional use of a specially developed edge enhancement oper-ator, termed a 'moat operator'. Details of these methods have been published previously [31].

Extraction of candidate lesion features

For each candidate lesion data were extracted to quantify numerically size, shape, hue and intensity.

Classification of candidate lesions as true lesion or noise by artificial neural network

All images were graded by the clinical research fellow, using a purpose written lesion-labelling program, which allowed identification and classification of each individual lesion in images from patients 1–500. The program output was a text file containing lesion co-ordinates and type (microaneurysm, haemorrhage, exudate, drusen and other). Lesion candidate features were used as inputs to an artificial neural network [32].

Classification of images and patients as normal or abnormal using mathematical rules

Each image was classified as normal or abnormal according to the presence or absence of lesions. A patient was classified as abnormal if either image was abnormal. Threshold settings allowing for one or more possible lesion identified by the neural network to be counted as normal were evaluated for both haemorrhages and microaneurysms (HMA > 0, HMA > 1, etc.) and exudates (EX > 0, etc.).

System evaluation

The trained system was evaluated using the previously unseen images from patients 501–1273. System results were compared with the human grading by image and by patient. True-positive, true-negative, false-positive and false-negative results were obtained, allowing calculation of sensitivity, specificity, positive predictive value (PPV) and negative predictive value (NPV). Confidence intervals at the 95% limits where calculated for each measurement using the standard theory of proportions where the standard error was equal to the square root of $[p \times (1 - p)/n]$ where p = sensitivity, specificity, PPV or NPV expressed as fractions, and n = the total number of observations.

Results

Excluding ungradable images, sensitivity and specificity for detection of any retinopathy on an image by image and a patient by patient basis using the 773 evaluation patients are summarized in Tables 2 and 3, respectively. There were 605 females (48%) and 665 males (52%); for two patients sex was unknown. Ethnic data were available for only 577 patients, consisting of 63 Asian (9%), 173 black (25%), 442 white (64%) and 15 other races (2%). The range of results obtained by varying the classification rules applied is shown.

Where retinopathy lesions were missed in one image the patient was frequently flagged as abnormal as a result of lesions detected in the opposite eye.

An example of feature detection in an image is shown in Fig. 1.

Using the detection of any exudates and any haemorrhages/microaneurysms in either eye of a patient provided a sensitivity of 95.1% (95% confidence interval 92.3, 97.7) and specificity of 46.3% (41.6, 51.0) with no sight-threatening retinopathy missed. Using the detection of any exudates and four or more haemorrhages/microaneurysms in either eye of a patient provided a sensitivity of 79.0% (74.1, 83.9) and specificity of 69.5% (65.2, 73.8) with four patients with sight-threatening retinopathy missed. Receiver operator coefficient curves are shown in Fig. 2. The predictive power of the system for the detection of DR is illustrated by the points which are

Table 2 Detection of retinopathy by image

Classification rule:	HMA > 0 & EX > 0	HMA > 1 & EX > 0	HMA > 2 & EX > 0	HMA > 3 & EX > 0	HMA > 4 & EX > 0
Total gradable images	1406	1406	1406	1406	1406
Images with DR present by grader	427 (30.4%)	427 (30.4%)	427 (30.4%)	427 (30.4%)	427 (30.4%)
Images with DR present by system	748 (53.2%)	695 (49.4%)	586 (41.7%)	562 (40.0%)	504 (35.8%)
True positives	380 (27.0%)	373 (26.5%)	340 (24.2%)	333 (23.7%)	304 (21.6%)
True negatives	611 (43.5%)	657 (46.7%)	733 (52.1%)	750 (53.3%)	779 (55.4%)
False positives	368 (26.2%)	322 (22.9%)	246 (17.5%)	229 (16.3%)	200 (14.2%)
False negatives	47 (3.3%)	54 (3.8%)	87 (6.2%)	94 (6.7%)	123 (8.7%)
Sensitivity for any retinopathy	89.0% (86.0, 92.0)	87.3% (84.2, 90.5)	79.6% (75.8, 83.4)	78.0% (74.1, 81.9)	71.2% (66.9, 75.5)
Specificity for any retinopathy	62.4% (59.4, 65.4)	67.1% (64.2, 70.1)	74.8% (72.2, 77.6)	76.6% (74.0, 79.3)	79.6% (77.0, 82.1)
Positive predictive value	0.51 (0.47, 0.54)	0.54 (0.50, 0.57)	0.58 (0.54, 0.62)	0.59 (0.55, 0.63)	0.60 (0.56, 0.65)
Negative predictive value	0.93 (0.91, 0.95)	0.92 (0.90, 0.94)	0.89 (0.87, 0.91)	0.89 (0.87, 0.91)	0.86 (0.84, 0.89)
Number of IMAGES with sight-threatening retinopathy missed	5 (0.4%)	5 (0.4%)	5 (0.4%)	5 (0.4%)	9 (0.6%)

Each image was used as an individual variable for analysis.
DR, Diabetic retinopathy; HMA, haemorrhages/microaneurysms; EX, exudates. 95% confidence intervals are provided for sensitivity, specificity and predictive values.

Table 3 Detection of retinopathy by patient

Classification rule:	HMA > 0 & EX > 0	HMA > 1 & EX > 0	HMA > 2 & EX > 0	HMA > 3 & EX > 0	HMA > 4 & EX > 0
Total patients with full set of gradable images	703	703	703	703	703
Patients with DR present by grader	267 (38.0%)	267 (38.0%)	267 (38.0%)	267 (38.0%)	267 (38.0%)
Patients with DR present by system	488 (69.4%)	459 (65.3%)	398 (56.6%)	385 (54.8%)	344 (48.9%)
True positives	254 (36.1%)	253 (36.0%)	236 (33.6%)	232 (33.0%)	211 (30.0%)
True negatives	202 (28.7%)	230 (32.7%)	274 (39.0%)	283 (40.3%)	303 (43.1%)
False positives	234 (33.3%)	206 (29.3%)	162 (23.0%)	153 (21.8%)	133 (18.9%)
False negatives	13 (1.8%)	14 (2.0%)	31 (4.4%)	35 (5.0%)	56 (8.0%)
Sensitivity for any retinopathy	95.1% (92.5, 97.7)	94.8% (92.1, 97.4)	88.4% (84.5, 92.2)	86.9% (82.3, 90.9)	79.0% (74.1, 83.9)
Specificity for any retinopathy	46.3% (41.6, 51.0)	52.8% (48.1, 57.4)	62.8% (58.3, 67.4)	64.9% (60.4, 69.4)	69.5% (65.2, 73.8)
Positive predictive value	0.52 (0.48, 0.56)	0.55 (0.51, 0.60)	0.59 (0.54, 0.64)	0.60 (0.55, 0.65)	0.61 (0.56, 0.66)
Negative predictive value	0.94 (0.91, 0.97)	0.94 (0.91, 0.97)	0.90 (0.86, 0.93)	0.89 (0.86, 0.92)	0.84 (0.81, 0.88)
Number of patients with sight-threatening retinopathy missed	0	0	1 (0.1%)	1 (0.1%)	4 (0.6%)

Data from right and left eyes from each patient were combined to allow analysis for the detection of retinopathy.
DR, Diabetic retinopathy; HMA, haemorrhages/microaneurysms; EX, exudates. 95% confidence intervals are provided for sensitivity, specificity and predictive values.

approaching the top left of the graph (top left corner indicates 100% sensitivity and specificity).

Threshold settings requiring more than one exudate type lesion per image (EX > 1) for the definition of abnormality resulted in a similar range of sensitivity and specificity for the detection of any retinopathy but a considerable increase in the number of patients with sight-threatening retinopathy missed by the system. Four sight-threatened patients would be missed at the HMA > 0/EX > 1 setting.

The number of patients in the evaluation set with ungradable images was 70 (9.1%) out of 773. Drusen accounted for a significant proportion of the false-positive results; of the 206 false-positive patients at the HMA > 1/EX > 0 setting 94 (45.6%) had drusen.

Discussion

In this study, computer-based algorithms were used to pre-process retinal digital images, localize the major retinal landmarks and recognize diabetic pathologies, without any intervention from an operator. We have previously described a variety of techniques employed in image pre-processing and identification of normal features such as the optic disc, fovea, retinal blood vessels, and abnormal features such as exudates, microaneurysms and haemorrhages. The detection of these features has been highly effective but gives little indication of the efficacy of these algorithms in clinical practice. In this study we have evaluated a system utilizing these methods for the detection of diabetic retinopathy in the screening environment.

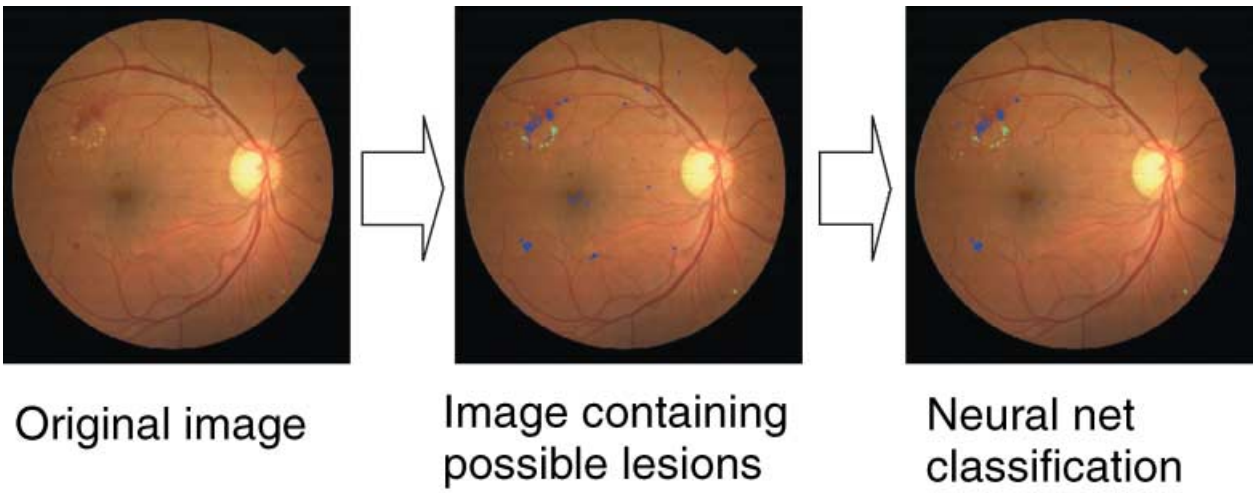

Figure 1 A selected image demonstrating the detection of haemorrhages/microaneurysms (blue) and exudates (green).

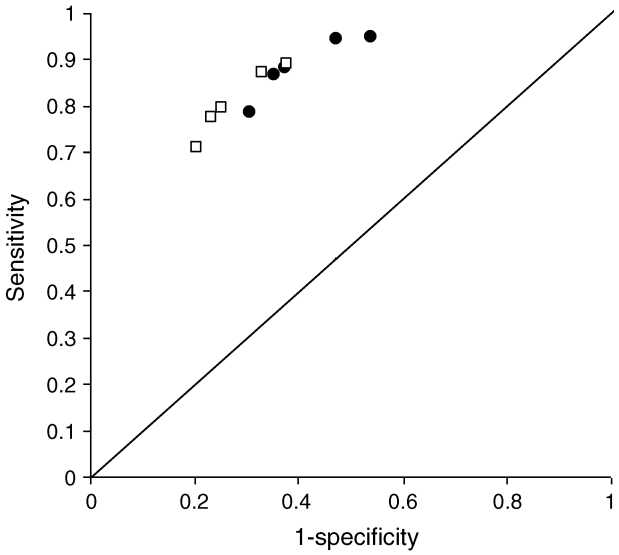

Figure 2 The predictive power of the system for the detection of diabetic retinopathy is illustrated by the points which are approaching the top left of the graph (top left corner indicates 100% sensitivity and specificity and the diagonal line no predictability of the test). ●, Patient; □, image.

By setting appropriate parameters it is possible to obtain a sensitivity of 94.8% (92.1, 97.4) and a specificity of 52.8% (48.1, 57.4) for the detection of DR, maximizing specificity without missing sight-threatening DR. The workload of a screener would be reduced by a third and the number of patients examined without diabetic retinopathy reduced by over a half.

Using an automated method it was possible to select those images with high probability of abnormality without missing sight-threatening disease. A grader would be able to view a preselected cohort of images to grade the retinopathy and determine the urgency of referral for treatment. The images were directly extracted from an active screening program; therefore the system was tested on images of variable quality typical of a screening program. Even so, the results were comparable to those received using microaneurysm detection in high-resolution red-free images [22]. However, such images are not routinely utilized in diabetic screening and would require human graders to retrain if applied to screening programs. Taking both red-free and colour images is undesirable because this would increase the costs both in time and money and considerably increase the storage requirements for digital images. In addition, our data suggest that omission of detection of exudates causes patients with sight-threatening retinopathy to be missed. Higher resolution cameras are becoming more widely available. It is expected that higher resolution images will aid detection of small lesions such as microaneurysms, thereby potentially improving the efficiency of the system.

The south London population has a wide mixture of races. The system had to cope with the subsequent variation in the pigmentation of the fundus. This is relevant because countries with populations of increased pigmentation are experiencing the greatest increase in the incidence of diabetes.

The high prevalence of other conditions, particularly age-related macular degeneration, resulted in a reduced specificity for the detection of diabetic retinopathy. This reflects our elderly patient group. Any screening tool should err on the side of sensitivity to avoid missing patients who are at risk. As a first point of triage of the screened population a loss of specificity, although undesirable, is less important.

In our study few eyes had preproliferative or proliferative disease. These were detected by the system because other retinopathy features were also present. The numbers of patients were too small for a meaningful analysis of the risk of missing an individual with proliferation. This may limit the implementation of software-based grading of sight-threatening retinopathy, unless peripheral retinal ischaemia can be implied from the widespread presence of other retinal lesions. More evaluation of this issue will be needed.

In our population 38% of the patients had retinopathy and would have required grading by an experienced observer. Of the rest at least half with no retinopathy were removed by the system leaving the remainder to be examined, a high proportion of whom had images with age-related macular degeneration, myopia or other abnormalities common in the screened population. Overall the workload of a grader would have been reduced by over a third, with considerable cost benefits.

Diabetes UK guidelines recommend a minimum standard of 80% sensitivity and 95% specificity of detection of sight-threatening diabetic retinopathy by any method. In their health policy model, Javitt *et al*. suggested that a sensitivity of 60% or greater maximized cost effectiveness in screening for diabetic retinopathy [33]. Increasing screening sensitivity from 60% to 100% provided little additional benefit due to the frequency of screening and the likelihood that retinopathy cases missed at one visit will be detected at the next. The results presented here indicate that if the computerized system was used in combination with a grader, these targets might be met, the computer system providing high sensitivity and the grader providing the required specificity. The system could therefore be applied to any screening program employing digital photographic imaging. The system does not replace the human grader but acts as a filter of normal images, thereby reducing workload. In the process only a few patients with DR and none with sight-threatening disease would not be examined by the grader.

Further investigation should improve the efficiency of the model. Development and implementation of a method for automatically identifying ungradable images may be the most important next step. Other work will involve the application of the algorithms to higher resolution images; more images of each eye and image registration. Distinguishing drusen from exudates may prove difficult as human graders often have difficulty with this. The specific detection of sight-threatening maculopathy is also achievable, e.g. the software is able to correctly identify the fovea in 84.5% of cases, therefore there is potential to superimpose a perifoveal mask to examine for hard exudates in this area.

In conclusion, with further development the automated detection of DR could become a highly effective way of reducing the burden on screening services by filtering out normal images, allowing the screener to classify only those images with a high chance of abnormality. This has major implications for the reduction of cost and improvement of efficiency of a diabetic screening program employing digital retinal images.

Acknowledgements

The authors are grateful to Steve Carey and Shirley Smith of the Department of Medicine, St Thomas' Hospital, London for providing the images and to the Special Trustees of St George's Hospital, The Lions Sight-First Diabetic Retinopathy Research Program of the American Diabetes Association and the IRIS Fund for the Prevention of Blindness for funding.

References

1 Evans J, Rooney C, Ashgood S, Dattan N, Wormald R. Blindness and partial sight in England and Wales April 1900–March 1991. *Health Trends* 1996; **28**: 5–12.
2 Diabetic Retinopathy Study. Photocoagulation treatment of proliferative diabetic retinopathy: the second report of Diabetic Retinopathy Study findings. *Ophthalmology* 1978; **85**: 82–106.
3 Early Treatment Diabetic Retinopathy Study Research Group. Early photocoagulation for diabetic retinopathy. ETDRS report number 9. *Ophthalmology* 1991; **98**: 766–785.
4 Clements C. National screening programme for diabetic retinopathy. Digital image may be better for screening. *Br Med J* 2002; **324**: 849–850.
5 Henricsson M, Karlsson C, Ekholm L, Kaikkonen P, Sellman A, Steffert E *et al.* Colour slides or digital photography in diabetes screening—a comparison. *Acta Ophthalmol Scand* 2000; **78**: 164–168.
6 Kerr D, Cavan DA, Jennings B, Dunnington C, Gold D, Crick M. Beyond retinal screening: digital imaging in the assessment and follow-up of patients with diabetic retinopathy. *Diabet Med* 1998; **15**: 878–882.
7 Liesenfeld B, Kohner E, Piehlmeier W, Kluthe S, Aldington S, Porta M *et al.* A telemedical approach to the screening of diabetic retinopathy: digital fundus photography. *Diabetes Care* 2000; **23**: 345–348.
8 Lin DY, Blumenkranz MS, Brothers R. The role of digital fundus photography in diabetic retinopathy screening. Digital Diabetic Screening Group (DDSG). *Diabetes Technol Ther* 1999; **1**: 477–487.
9 Maberley D, Cruess AF, Barile G, Slakter J. Digital photographic screening for diabetic retinopathy in the James Bay Cree. *Ophthalmic Epidemiol* 2002; **9**: 169–178.
10 Robbins AS, Hurley LD, Dudenhoefer EJ, Chao SY. Performance characteristics of digital fundus photography as a screening test for diabetic retinopathy in a low-risk population. *Diabetes Technol Ther* 2001; **3**: 193–200.
11 Scanlon P. Digital retinal photography in diabetic eye screening. *Diabetes Technol Ther* 2001; **3**: 187–191.
12 Scanlon P. Screening for diabetic retinopathy by digital imaging photography and technician ophthalmoscopy. *Diabetes Technol Ther* 2000; **2**: 283–287.
13 Taylor DJ, Jacob JS, Tooke JE. The integration of digital camera derived images with a computer based diabetes register for use in retinal screening. *Comput Meth Programs Biomed* 2000; **62**: 157–163.
14 Taylor DJ, Fisher J, Jacob J, Tooke JE. The use of digital cameras in a mobile retinal screening environment. *Diabet Med* 1999; **16**: 680–686.
15 Yogesan K, Constable IJ, Eikelboom RH, van Saarloos PP. Teleophthalmic screening using digital imaging devices. *Aust NZ J Ophthalmol* 1998; **26**: S9–11.
16 Taylor R. Practical community screening for diabetic retinopathy using the mobile retinal camera: report of a 12 centre study. *Diabet Med* 1996; **13**: 946–952.
17 Bjorvig S, Johansen MA, Fossen K. An economic analysis of screening for diabetic retinopathy. *J Telemed Telecare* 2002; **8**: 32–35.
18 Lairson D, Pugh J, Kapadia AS, Lorimor RJ, Jacobson J, Velez R. Cost effectiveness of alternative methods for diabetic retinopathy screening. *Diabetes Care* 1992; **15**: 1369–1377.
19 Cree MJ, Olson JA, McHardy KC, Sharp PF, Forrester JV. A fully automated comparative microaneurysm digital detection system. *Eye* 1997; **11**: 622–628.
20 Hipwell JH, Strachan F, Olson JA, McHardy KC, Sharp PF, Forrester JV. Automated detection of microaneurysms in digital red-free photographs: a diabetic retinopathy screening tool. *Diabet Med* 2000; **17**: 588–594.
21 Phillips RP, Spencer T, Ross PG, Sharp PF, Forrester JV. Quantification of diabetic maculopathy by digital imaging of the fundus. *Eye* 1991; **5**: 130–137.

22 Spencer T, Olson JA, McHardy KC, Sharp PF, Forrester JV. An image-processing strategy for the segmentation and quantification of microaneurysms in fluorescein angiograms of the ocular fundus. *Comput Biomed Res* 1996; **29**: 284–302.
23 Spencer T, Phillips RP, Sharp PF, Forrester JV. Automated detection and quantification of microaneurysms in fluorescein angiograms. *Graefes Arch Clin Exp Ophthalmol* 1992; **230**: 36–41.
24 Gardner GG, Keating D, Williamson TH, Elliott AT. Automatic detection of diabetic retinopathy using an artificial neural network: a screening tool. *Br J Ophthalmol* 1996; **80**: 940–944.
25 Ege BM, Hejlesen OK, Larsen OV, Moller K, Jennings B, Kerr D *et al.* Screening for diabetic retinopathy using computer based image analysis and statistical classification. *Comput Meth Programs Biomed* 2000; **62**: 165–175.
26 Lee S, Lee E, Kingsley R, Wang Y, Russell D, Klein R *et al.* Comparison of diagnosis of early retinal lesions of diabetic retinopathy between a computer and human experts. *Arch Ophthalmol* 2001; **119**: 509–515.
27 Newsom RS, Sinthanayothin C, Boyce J, Casswell AG, Williamson TH. Clinical evaluation of 'local contrast enhancement' for oral fluorescein angiograms. *Eye* 2000; **14**: 318–323.
28 Sjolie AK, Stephenson J, Aldington S, Kohner E, Janka H, Stevens L *et al.* Retinopathy and vision loss in insulin-dependent diabetes in Europe. The EURODIAB IDDM Complications Study. *Ophthalmology* 1997; **104**: 252–260.
29 Sinthanayothin C, Boyce JF, Cook HL, Williamson TH. Automated localisation of the optic disc, fovea, and retinal blood vessels from digital colour fundus images. *Br J Ophthalmol* 1999; **83**: 902–910.
30 Hoover A, Kouznetsova V, Goldbaum M. Locating blood vessels in retinal images by piecewise threshold probing of a matched filter response. *IEEE Trans Med Imaging* 2000; **19**: 203–210.
31 Sinthanayothin C, Boyce JF, Williamson TH, Cook HL, Mensah E, Lal S *et al.* Automated detection of diabetic retinopathy on digital fundus images. *Diabet Med* 2002; **19**: 105–112.
32 Haykin S. *Neural Networks: A Comprehensive Foundation*, 2nd edn. Englewood Cliffs, NJ: Prentice Hall, 1999.
33 Javitt JC, Aiello LP, Bassi LJ, Chiang YP, Canner JK. Detecting and treating retinopathy in patients with type I diabetes mellitus. Savings associated with improved implementation of current guidelines. American Academy of Ophthalmology. *Ophthalmology* 1991; **98**: 1565–1573.